13th World Conference on Earthquake Engineering
Vancouver, B.C., Canada
August 1-6, 2004
Paper No. 1369

EVALUATION ON THE SHEAR STRENGTHENING EFFECT OF RC COLUMNS WITH CARBON FIBER SHEETS

Yong-Taeg LEE[1], Seung-Hun KIM[2], Hong-Soon HWANG[1], Li-Hyung LEE[3]

SUMMARY

This study described the experimental and analytical works to investigate the structural behavior and shear retrofit performance of reinforced concrete (RC) columns with carbon fiber sheets (CFS). Experimental works were conducted for five specimens varied in the reinforcement quantity and adhesion method of CFS. Throughout cyclic test, the strength, stiffness, failure modes, ductility, and energy dissipation capacity were discussed. As analytical works, FEM analysis was performed. The material composition model of CFS and bond model between concrete and CFS are proposed and applied to the analysis. The test and analysis results showed that the increase of the CFS quantity improved the ductility and energy dissipation capacity and changed shear failure mode into flexural failure mode.

INTRODUCTION

Failure of RC columns, subjected to cyclic lateral loads by earthquake, can be due to insufficiency in shear strength, in flexural strength, or ductility. The most undesirable mode of failure is shear failure. Column shear failure is possible if the transverse reinforcement in the column is poorly detailed or inadequately anchored. CFS(Carbon Fiver Sheets) can enhance both the shear capacity and ductility of columns.(Teng [1]) Shear retrofit methods using CFS are popular because of its properties such as anti-corrosiveness, lightweight, and workability.

The objective of this research was to evaluate the structural behavior and shear retrofit performance of RC column with CFS from the experimental and analytical works. Experimental works were conducted for five specimens varied in the reinforcement quantity and adhesion method of CFS. Throughout cyclic test, the strength, stiffness, failure modes, ductility, and energy dissipation capacity were discussed. Test results are compared with FEM analysis results.

EXPERIMENTAL PROGRAM

Specimens

Five column specimens of an approximately 1/3 scale were tested. Fig. 1 shows the cross-sections of specimens and shapes. The column height of all specimens was 900 mm and the original cross-section was 350 mm in width (B) and 350 mm in depth (D). The critical moment-to-shear span ratio (M/QD) was 1.5.

[1] Professor, Hanbat National University, Daejeon, Korea. Email : ytlee@hanbat.ac.kr
[2] Research Assistant Professor, STRESS, Hanyang University, Seoul, Korea
[3] Professor, Hanyang University, Seoul, Korea

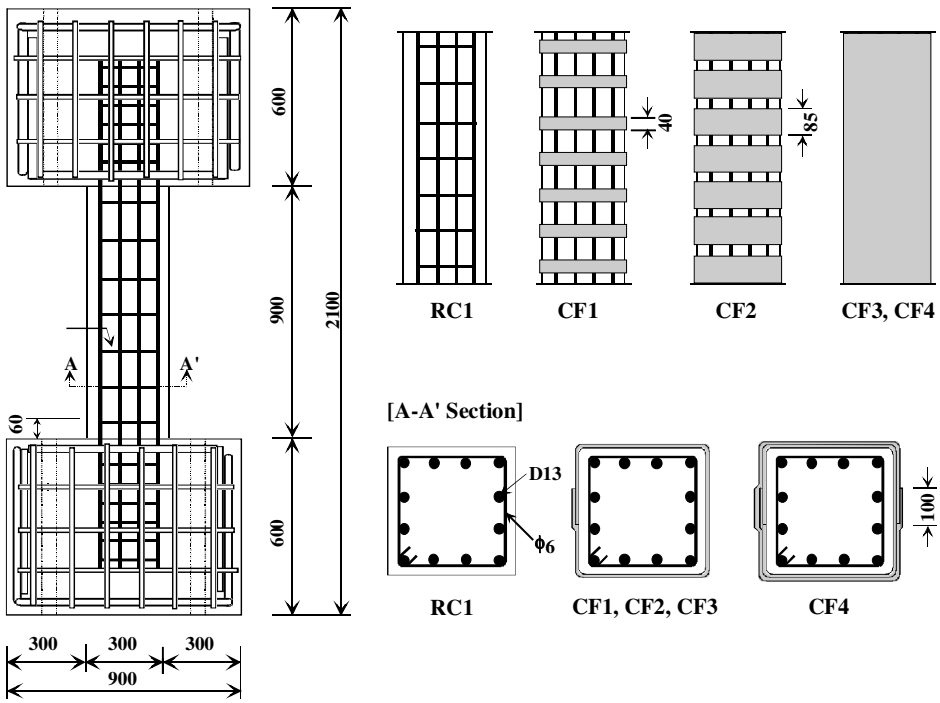

Fig. 1 Cross-sections of specimens and shapes (Unit; mm)

Specimen RC1 is a prototype column without strengthening by CFS. The longitudinal reinforcing bars of all specimens were 12-D13 (reinforcement ratio: 1.69%). Hoop was 2- ϕ6 @100 (reinforcement ratio : 0.151%). Specimens CF1 and CF2 were retrofitted with CFS, of which the widths were 40 mm and 85 mm, at the centerline of hoop, respectively. Specimens CF3 and CF4 were horizontally wrapped with one and two layers of CFS about column, respectively. The length of the overlapped CFS was 100 mm in each layer.

Material properties

The compressive strength of concrete on the testing date was 35.3 Mpa. All the reinforcements steel used in the specimens conformed to KS SD40. Mechanical properties of the reinforcing bars and CFS are listed in Table 1.

Table 1 Mechanical properties of the reinforcing bars and CFS

Type	Elastic modulus (N/mm^2)	Yield strength (N/mm^2)	Yield strain ($*10^{-6}$)	Tensile strength (N/mm^2)	Extensibility (%)
ϕ6	195219	721	3701	795	25.3
D13	167751	455	2708	636	19.2
CFS	230535	3483	15000	-	-

Test setup and loading

The full-scale model column was subjected to a constant axial load and cyclic lateral forces. The lateral loading system displaces the column in a double-curvature condition with the point of inflection occurring at its mid-height, as schematically shown in Fig. 2. An 'L'-shape loading arm connects the load stub of the column to a 1000 kN pseudo-controlled actuator positioned at the column mid-height. The axial load was applied by two 250 kN pseudo-controlled actuators along the axis of the column.

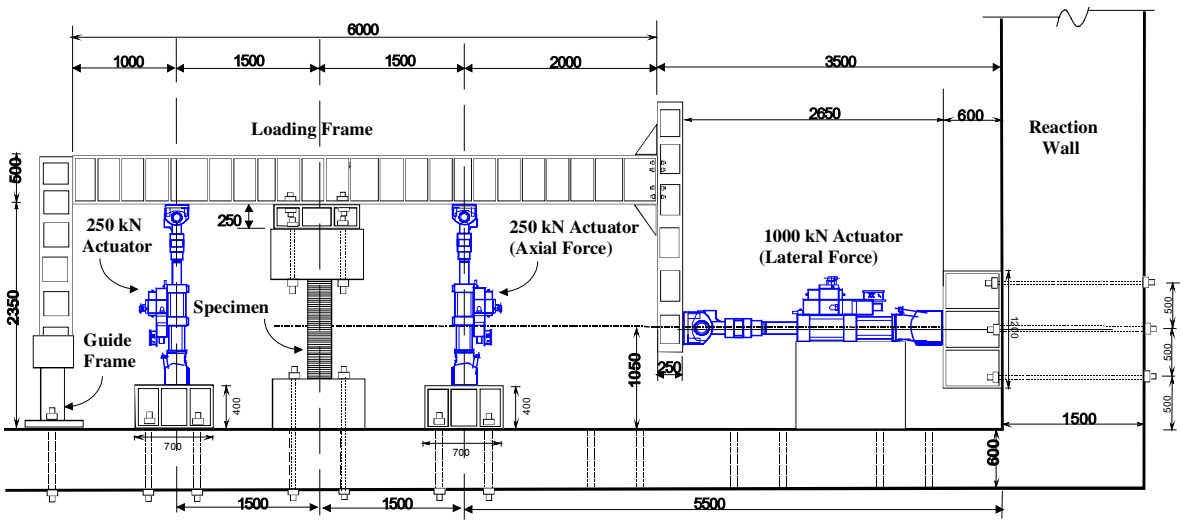

Fig. 2 Test setup

Cyclic shear force was applied to the column while the axial compressive load was held constant. The axial compressive load applied to all the specimens was 477 kN. This axial load corresponded to the axial stress of 15% of the concrete compressive strength of specimen RC1. Cyclic shear force was controlled by defection angle of the column, R =δ/h ; where δ is the horizontal displacements of the upper end og column and h(=900 mm) is the column height. Fig. 3 shows lateral cyclic loading patterns.

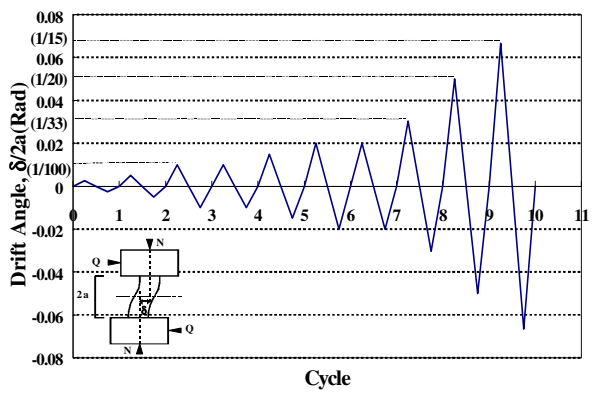

Fig. 3 Cyclic loading patterns

TEST RESULTS

Failure patterns

Fig. 4 shows failure patterns of all specimens. In specimen RC1, initial shear cracks occurred at R=1/200 rad. The maximum strength was reached at R=1/100 rad with buckling of longitudinal reinforcing bars and shear failure of column. In specimen CF1, initial shear cracks occurred at R=1/200 rad, and failure at R=1/33 with fracture of CFS. A similar crack process was also observed for specimen CF2. In specimen CF3 and CF4, bulging of CFS was observed until R=1/33. With rupture of CFS, specimen CF3 and CF4 failed at R=1/20 and 1/15, respectively.

Lateral force-displacement responses and shear strengths

The lateral force-displacement hysteretic responses for all specimens are shown in Fig. 5. In specimen RC1, the hysteresis loops showed the shape of a typical pure shear failure.

(a) RC1 (b) CF1 (c) CF2 (d) CF3 (e) CF4

Fig. 4 Failure patterns

The maximum shear strength was 198.2 kN in the positive loading direction. The average of the maximum shear strengths of retrofitted RC columns was 269.8 kN, which was 1.36 times as large as the maximum shear strength of RC1. In specimen CF4, yielding of longitudinal bar occurred before the peak strength. It showed the flexural yielding of RC column. As increasing of CFS quantity, the degradation of the load-carrying capacity upon the cycling at a given peak displacement was smaller and the hysteresis loops was more stable.

The yield shear strengths, maximum strengths, and strengths at yielding point of longitudinal bar for all specimens are compared in Table 2.

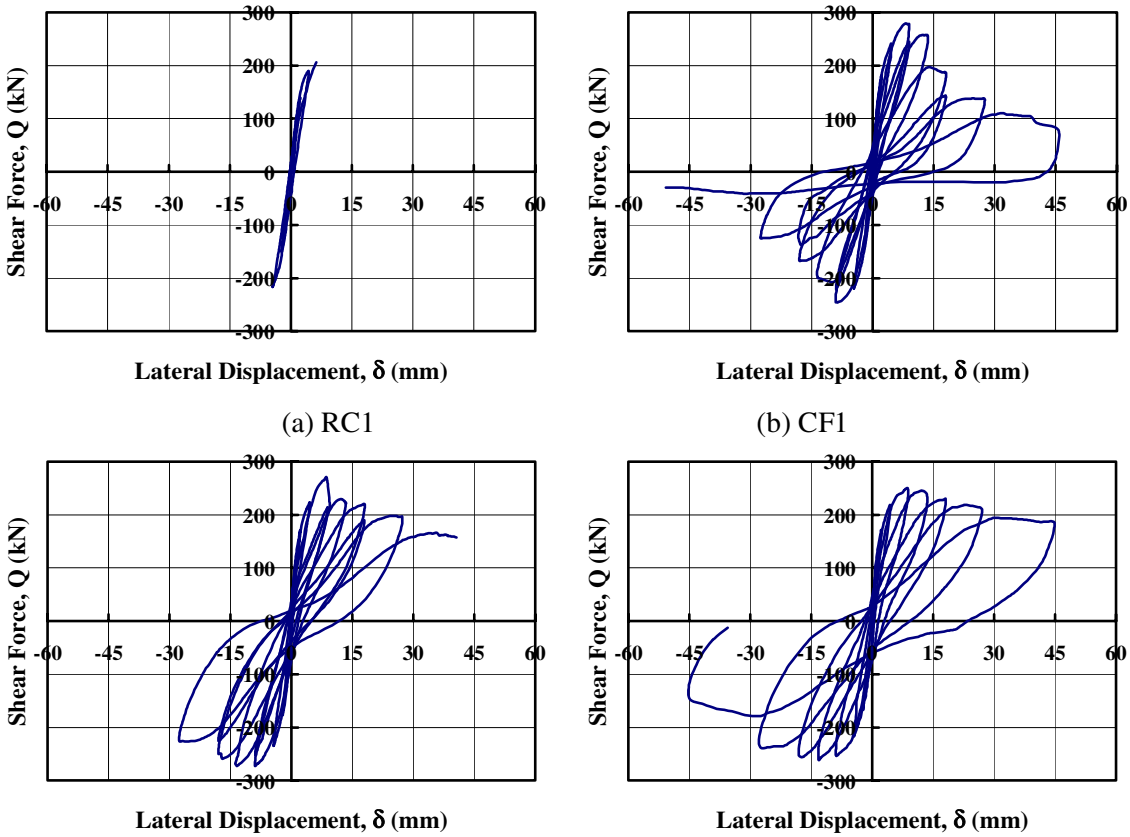

(a) RC1 (b) CF1

(c) CF2 (d) CF3

Fig. 5 Lateral force-displacement responses

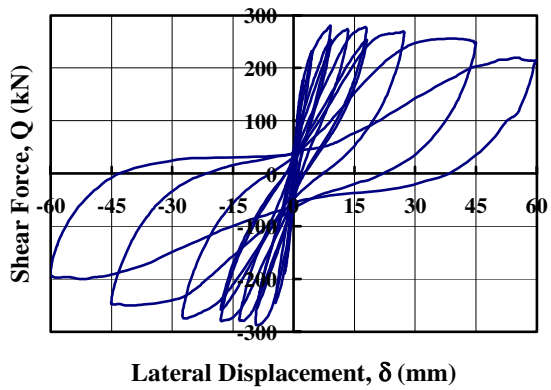

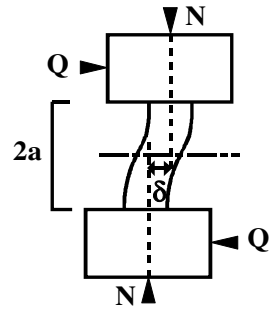

(e) CF4

Fig. 5 Lateral force-displacement responses (continued)

Table 2 Comparison of Shear Strengths

Specimen		Yielding of longitudinal bar		Yield Strength		Maximum Strength	
		Q_{By} (kN)	δ_{By} (mm)	Q_y (kN)	δ_y (mm)	Q_{max} (kN)	δ_{max} (mm)
RC1	+	*	*	151.1	2.42	198.2	5.87
	-			-175.6	-2.67	-216.8	-4.47
CF1	+	279.6	8.12	209.0	3.00	279.6	8.12
	-			-190.3	-3.40	-245.3	-9.03
CF2	+	-266.8	-8.00	198.2	3.28	270.8	8.68
	-			-186.4	-2.69	-272.7	-13.75
CF3	+	-260.9	-13.20	180.5	2.75	249.2	8.80
	-			-197.2	-3.60	-260.9	-13.20
CF4	+	267.8	7.47	206.0	3.55	279.6	9.07
	-			-201.1	-2.78	-285.5	-9.32

Comparison of displacement ductility ratio and energy absorption capacity

The displacement ductility ratios (δ_u/δ_y) and energy absorption capacities (E) for all specimens are compared in Table 3. δ_u is the displacement at the point 80% maximum strength after peak strength.

The displacement ductility ratio and energy absorption capacity were very increased in proportion to CFS quantity. Their ratios of specimen CF4 and specimen RC1, of which the ratio of total shear reinforcement ratio was 5.7, were 7.8 and 17.0, respectively.

Table 3 Comparison of displacement ductility ratio and energy absorption capacity

Specimen	δ_u/δ_y	E (kN·mm)	$E / E_{CF\text{-}NO}$
RC1	2.13	772.0 (=$E_{CF\text{-}NO}$)	1
CF1	4.64	3214.7	4.16
CF2	8.06	5423.0	7.02
CF3	11.09	7652.8	9.12
CF4	16.52	13123.8	17.00

ANALYTICAL MODEL

Analytical model

For all specimens, FEM analysis was conducted. TOTAL-RC, nonlinear FEM program for reinforced concrete, was used. Static shear force was applied to the column subjected to the constant axial force. Fig. 6 shows the finite element mesh of RC1 specimen.

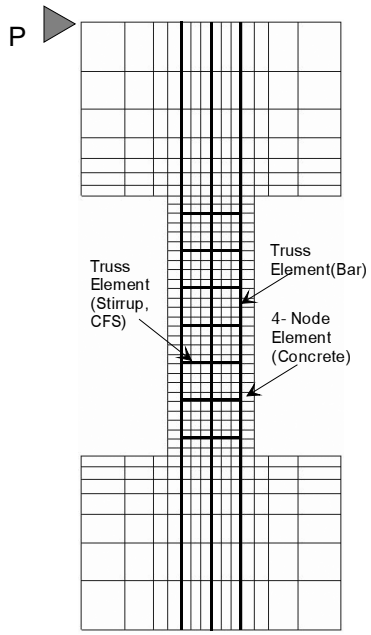

Fig. 6 Finite element mesh

Material model

Concrete

The concrete was modeled in a plate stress element of iso-parametric 4 nodes. For the maximum compressive strength of concrete, the kupfer's theory was used. The bi-linear model was used to consider the strain-softening after the maximum compressive strength. The tensile strength was assumed to be linearly elastic before the crack. After cracking, it was considered to the tensile-softening of exponent type. (Fig. 7 (a),(b))

Reinforcement

The steel was modeled as the truss element of two nodes and a yield condition of von-mieses was used. Plate bond element of iso-parametric 4 nodes was used to represent the bond between longitudinal bars and concrete. It was modeled in the property expressed by bi-linear. (Fig. 7 (c), (d))

CFS

The CFS was modeled in the truss element of 2 nodes. CFS was assumed as elastic before fracture. After fracture, it was released from stress. At the same time, the modulus of elasticity and tensile strength were decreased. Their magnitude were referred to the previous study results. (Fig. 7 (e))

Bond of concrete and CFS

Plate bond element of iso-parametric 4 nodes was used to represent the bond between CFS and concrete. The value of property was referred to the empirical formulas proposed from experimental results. (Fig. 7 (f))

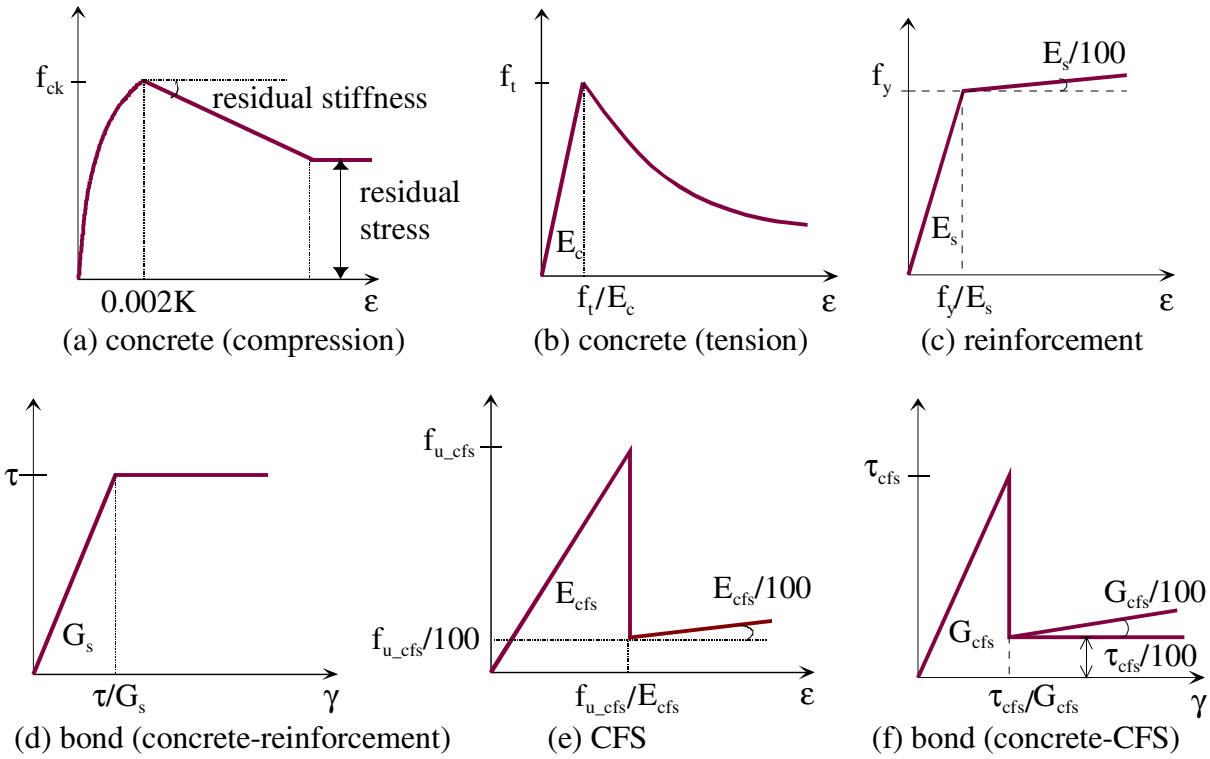

Fig. 7 Material model

ANALYTICAL RESULTS

Crack patterns and principal axial stress distribution

Fig. 8 shows the crack pattern and principal axial stress distribution of specimen CF1 from FEM analysis. Deformation of specimen CF1 by loading procedure is shown in Fig. 9. The principal axial stresses are concentrated at diagonal line of column. Flexural cracks and shear diagonal cracks appeared at the both ends of column. These crack patterns are similar to test results.

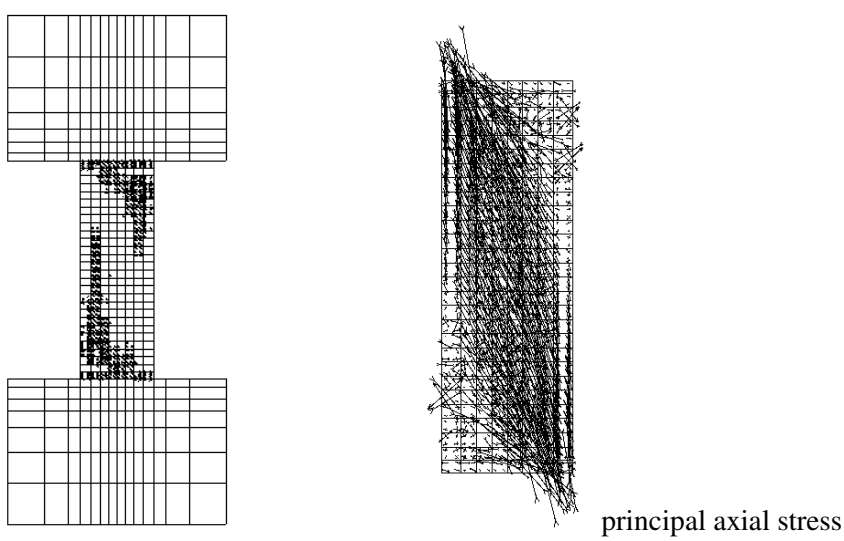

Fig. 8 Crack pattern and principal axial stress distribution of specimen CF1

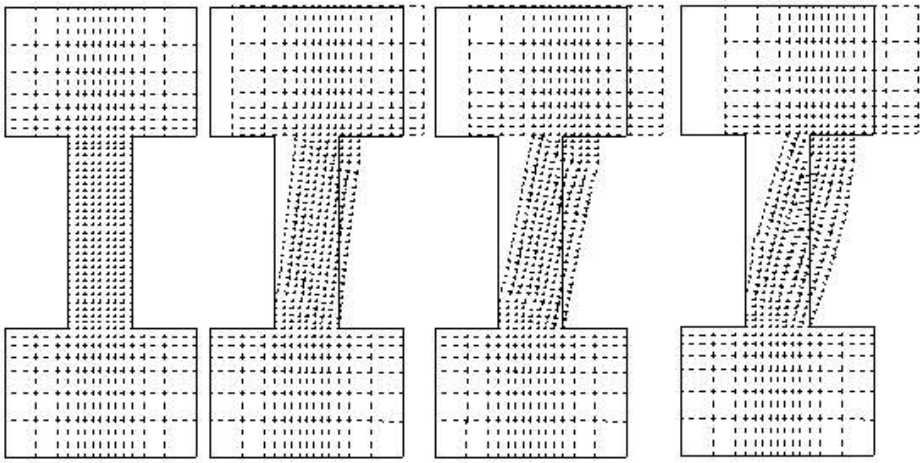

Fig. 9 Deformation of specimen CF1 by loading procedure

Lateral force-displacement responses

Analytical and experimental lateral force-displacement relations are compared in Fig. 10. Analysis overestimated loading capacity and stiffness. Amount of CFS didn't have effect on the increase of shear strength and stiffness. However, prediction of ductility was nearly accurate. The analysis results showed that the increase of the CFS quantity improved the ductility. For the increase of shear strength by the confine-effect of CFS, 3D FEM analysis will be suitable.

Strains of hoop reinforcement and CFS

Fig. 11 shows the strain of the second hoop reinforcement and CFS from the upper end of column. The strain shape of hoop reinforcement looked closer to CFS. In test and FEM analysis results, strains of hoop and CFS were very increased after yielding of column.

CONCLUSIONS

Experimental and analytical works were conducted to investigate the structural behavior and shear retrofit performance of RC columns with CFS. Several observations from this research are as followings.

(1) Retrofitting method with CFS can increase the shear strength, ductility, and energy dissipation capacity of RC column and change failure mode from shear failure into flexural failure.

(2) As increasing of CFS quantity, the degradation of the load-carrying capacity upon the cycling at a given peak displacement was smaller and the hysteresis loops was more stable.

(3) FEM model, using the improved composition model of CFS and bond model, is effective to predict the behavior of the column retrofitted with CFS, especially the ductile behavior.

ACKNOWLEDGEMENTS

The research described in this paper has been funded by STRESS Center and Sang Young Engineering. Co., Ltd.. The authors thank for this positive support.

REFERENCES

1. J. G. Teng, J. F. Chen, S. T. Smith, L. Lam, "FRP Strengthened RC Structures", John Wiley & Sons, LTD, 2002

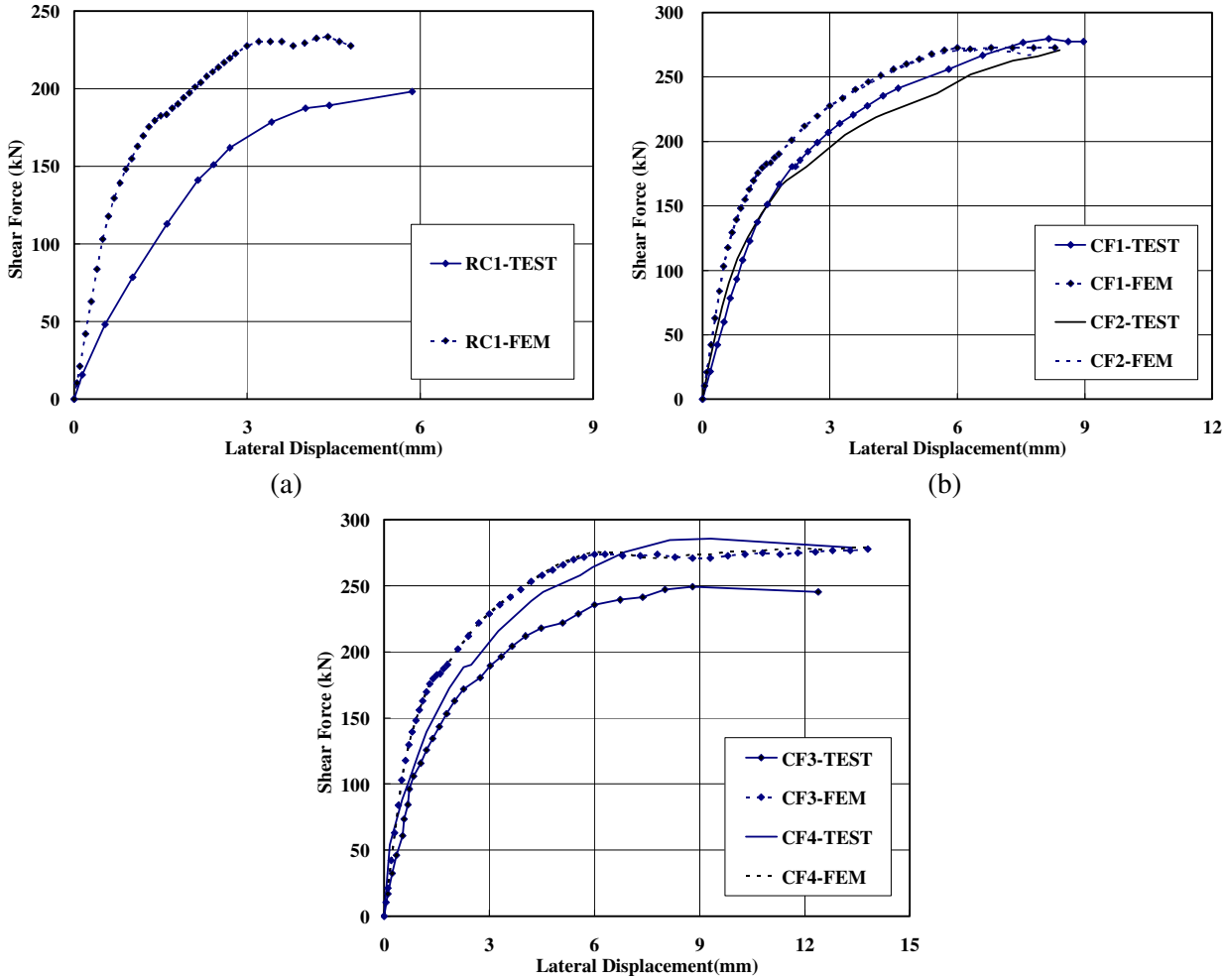

Fig. 10 Comparison of test and analytical results

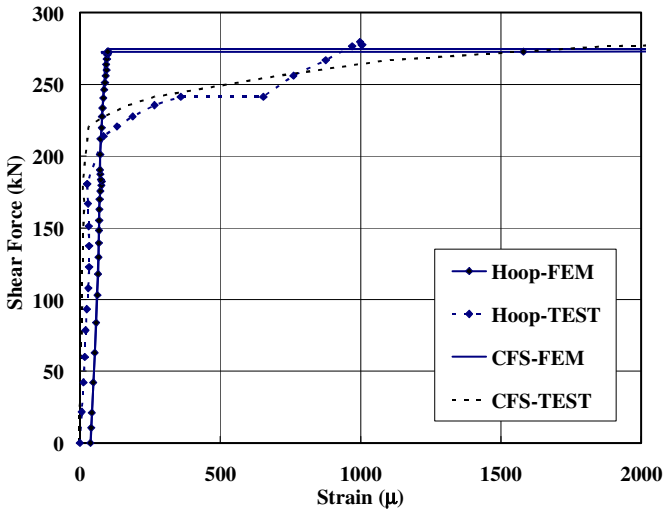

Fig. 11 Shear force-strain curve of hoop and CFS